Journal of Chromatography A, 1218 (2011) 4206–4212

Contents lists available at ScienceDirect

Journal of Chromatography A

journal homepage: www.elsevier.com/locate/chroma

Interactions and stability of silver nanoparticles in the aqueous phase: Influence of natural organic matter (NOM) and ionic strength

Markus Delay*, Tamara Dolt, Annette Woellhaf, Reinhard Sembritzki, Fritz H. Frimmel

Engler-Bunte-Institut, Chair of Water Chemistry, Karlsruhe Institute of Technology (KIT), Engler-Bunte-Ring 1, 76131 Karlsruhe, Germany

ARTICLE INFO

Article history:
Available online 4 March 2011

Dedicated to Russell F. Christman, pioneer of aquatic humic matter research.

Keywords:
Nanotechnology
Silver nanoparticles
Asymmetrical flow field-flow fractionation (AF^4)
Natural organic matter (NOM)

ABSTRACT

The rapid development of nanotechnology and the related production and application of nanosized materials such as engineered nanoparticles (ENP) inevitably lead to the emission of these products into environmental systems. So far, little is known about the occurrence and the behaviour of ENP in environmental aquatic systems. In this contribution, the influence of natural organic matter (NOM) and ionic strength on the stability and the interactions of silver nanoparticles (n-Ag) in aqueous suspensions was investigated using UV–vis spectroscopy and asymmetrical flow field-flow fractionation (AF^4) coupled with UV–vis detection and mass spectrometry (ICP-MS). n-Ag particles were synthesized by chemical reduction of $AgNO_3$ with $NaBH_4$ in the liquid phase at different NOM concentrations. It could be observed that the destabilization effect of increasing ionic strength on n-Ag suspensions was significantly decreased in the presence of NOM, leading to a more stable n-Ag particle suspension. The results indicate that this behaviour is due to the adsorption of NOM molecules onto the surface of n-Ag particles ("coating") and the resulting steric stabilization of the particle suspension. The application of AF^4 coupled with highly sensitive detectors turned out to be a powerful method to follow the aggregation of n-Ag particle suspensions at different physical–chemical conditions and to get meaningful information on their chemical composition and particle size distributions. The method described will also open the door to obtain reliable data on the occurrence and the behaviour of other ENP in environmental aquatic systems.

1. Introduction

Nanotechnology has become one of the most promising approaches to obtain new forms of materials. Typically, nanotechnology considers structures between approximately 1 and 100 nm in at least one dimension [1,2]. The properties of nanosized structures and engineered nanoparticles (ENP) are significantly different from those of bulk materials (macro scale) and can strongly be related to the nanometer scale of the substance, the large surface to mass ratio and to the surface properties of the components [3,4]. As a consequence, ENP show outstanding potential benefits for diverse industrial, medical, pharmaceutical, food, cosmetic, and life science applications [5–7]. Nanoscience enables the specific engineering of nanoparticles with defined material properties resulting in the production of a wide spectrum of ENP ranging from metal nanoparticles (e.g. Au, Ag), metal oxides (e.g. TiO_2, Fe_2O_3, Fe_3O_4, ZnO and SiO_2), quantum dots (e.g. CdTe, GaAs) to carbon based nanomaterials (e.g. black carbon, fullerenes, carbon nanotubes) (further details are given in [4–9]).

In particulate, there is an increasing number of products containing silver nanoparticles (n-Ag) leading to an estimated mass flow for n-Ag products in the range of some 100 t/a (for Europe) [10,11]. n-Ag particles are widely used as catalyst [12], in electronic applications [13], and in treatment of textiles due to their antimicrobial properties [14,15]. As a consequence, n-Ag particles will inevitably find their way into environmental systems. This is of high toxicological relevance as n-Ag has shown to have hazardous potential for the environment and human health [16,17].

Although numerous review articles on the environmental risk of ENP have been published recently, there is a severe lack of data on the actual production of ENP, on their occurrence and their behaviour in aqueous systems – their fate and ecological influence are widely unknown [18,19].

For a deeper understanding of the environmental behaviour of ENP in aquatic systems, it is of particular importance to identify and further develop analytical methods for their basic characterization and to investigate their fate in environmental matrices [9,20]. In this context, it is crucial to consider main water constituents (e.g. abundant cations such as sodium and calcium) as well as natural organic matter (NOM) which is ubiquitous in aquatic systems [21–23]. It is known from colloid sciences that NOM is likely to change the properties of ENP concerning their stability,

* Corresponding author. Tel.: +49 721 608 47059; fax: +49 721 608 47051.
E-mail address: markus.delay@kit.edu (M. Delay).

0021-9673/$ – see front matter © 2011 Elsevier B.V. All rights reserved.
doi:10.1016/j.chroma.2011.02.074

Table 1
Properties of the initial n-Ag suspensions in different matrices.

Sample name	ρ(DOC) in mg/L	pH value	Hydrodynamic diameter d_h in nm	Electrophoretic mobility in $m^2/(Vs)$ 10^{-8}	Zeta potential in mV
n-Ag/MQ	<0.1	8.7 ± 0.1	3.8 ± 1.1	−3.0 ± 0.1	−39 ± 1
n-Ag/MQ-HO26	9.0 ± 0.0	7.9 ± 0.1	9.8 ± 0.8	−2.4 ± 0.0	−30 ± 0
n-Ag/HO26	17.8 ± 0.1	7.8 ± 0.1	9.4 ± 1.1	−1.6 ± 0.1	−20 ± 1

their interactions with other water constituents, and their transport behaviour [24,25]. As an example, the presence of NOM might lead to a surface coating of the nanoparticles with NOM molecules. This adsorption of organic macromolecules onto (nano)particles is known to inhibit the coagulation potential of (nano)particle suspensions and thus to enhance their stability (steric stabilization) [26–29]. Especially with regard to water purification processes and human health protection, knowledge of these molecular interactions is of high relevance.

This contribution focuses on the interactions and stability of silver nanoparticles (n-Ag) in the aqueous phase, with the aim

(i) to follow the influence of the ionic strength on the aggregation behaviour, and
(ii) to study the effect of different NOM concentrations.

The methods used include UV–vis spectrometry and asymmetrical flow field-flow fractionation (AF^4) coupled with UV–vis detection and inductively-coupled plasma mass spectrometry (ICP-MS), UV–vis spectroscopy is a simple but powerful method to characterize n-Ag suspensions as n-Ag particles show plasmon absorption in the wavelength region λ = 390–420 nm [30–32]. Plasmon absorption is caused by the oscillation of free conduction electrons induced by an electromagnetic field [33]. For n-Ag particles, the plasmon peak shifts towards higher wavelengths with increasing particle radius [34]. For Ag-core nanoparticles coated with a dye an increase of the absorption peak wavelength could be observed when the thickness of the adsorbed dye layer increased [35].

Coupling of AF^4 with UV–vis and ICP-MS was shown to be well suited to provide simultaneous information on the particle size distribution and on the chemical composition of aqueous suspensions containing colloids or nanoparticles [9,36–38].

Benefits and limitations of these methods will be addressed as well as challenges for their further development to detect and characterize ENP in environmental samples.

2. Materials and methods

2.1. Preparation of n-Ag suspensions

n-Ag particles were directly synthesized in different liquid phases by chemical reduction of $AgNO_3$ with $NaBH_4$ according to Eq. (1) [31,39]:

$$2AgNO_3 + 2NaBH_4 + 6H_2O \rightarrow 2Ag + 2B(OH)_3 + 2NaNO_3 + 7H_2 \quad (1)$$

Stock solutions of $AgNO_3$ (ρ(Ag) = 1 g/L) and $NaBH_4$ ($c(NaBH_4)$ = 0.1 mol/L) were freshly prepared by dissolution of $AgNO_3$ and $NaBH_4$ (Merck, for analysis) in ultrapure water (Milli-Q, MQ; Millipore).

The different liquid phases used were:

(i) MQ water,
(ii) brown water from a bog lake (Lake Hohloh, HO26, Black Forest/Germany), and
(iii) a mixture of (i) and (ii) (volume ratio 1:1).

Corresponding sample names are: n-Ag/MQ for (i), n-Ag/HO26 for (ii), and n-Ag/MQ-HO26 for (iii).

Brown water from the Lake Hohloh is humic rich with 50–65% of humic substances (mass fraction of dissolved organic matter (DOC)), mainly containing C/H-substituted aromatic carbon and O-alkyl carbon [23]. Further details are given by Abbt-Braun et al. [40] and Frimmel et al. [23]. HO26 was filtrated before usage (0.45 μm, cellulose acetate; Millipore).

2.16 mL of the Ag stock solution were intensively mixed with 96.84 mL of the liquid phase in Teflon bottles (Nalgene). Subsequently, 1 mL of the $NaBH_4$ stock solution was added (total volume: 100 mL, c(Ag) = 0.2 mmol/L, $c(NaBH_4)$ = 1 mmol/L). The suspensions were intensively stirred magnetically in the closed bottles for 24 h.

2.2. Variation of ionic strength in the n-Ag suspensions

For investigating the stability of the n-Ag suspensions and their agglomeration behaviour at different ionic strengths, liquid solutions of $NaNO_3$ (Riedel-de Haën) or $Ca(NO_3)_2$ (Merck) were added to aliquots of the initial n-Ag suspensions, adjusting molar concentrations of Na^+ or Ca^{2+} of 1, 5, 10, and 50 mmol/L. Sodium and calcium were chosen as they are the most abundant monovalent and divalent cations in natural freshwaters, respectively [21] Concentration ranges applied were typical of natural surface waters [21,41].

2.3. Characterization of n-Ag suspensions

In order to characterize the n-Ag suspensions the following analytical methods and instruments were used:

- Dynamic light scattering (DLS) and laser Doppler electrophoresis (LDE) was applied to determine particle size distribution and zeta potential of the synthesized n-Ag suspensions using a Zetasizer Nano ZS (Malvern).
- UV–vis absorption spectroscopy was used to investigate the plasmon absorption of the suspensions and thus to get information on the stability of the suspensions and shifts of the plasmon peak at changing ionic strength. For this purpose, a UV–vis spectrophotometer (Cary 50, Varian) was employed.
- The concentration of dissolved organic carbon (DOC) in the suspensions was determined using a Total Organic Carbon Analyzer (TOC-V CSN, Shimadzu. Prior to measurement, samples were filtrated (0.45 μm, cellulose acetate filter, Millipore) and acidified with HNO_3 to remove inorganically bound carbon)
- AF^4 coupled with UV–vis detection and ICP-MS was employed to get information on the particle size distribution of the suspensions and on their chemical composition, and to follow in detail the aggregation behaviour of the suspensions when ionic strength was varied as described in Section 2.2. Details on the method are given in the next section.

2.4. Asymmetrical flow field-flow fractionation (AF^4)

For AF^4, a POSTNOVA HRFFF 10.000 system (postnova analytics, Munich/Germany) was used (eluent: $NaNO_3$ (5 mmol/L, pH ≈ 7); membrane: polyethersulfone (PES), molecular weight cut

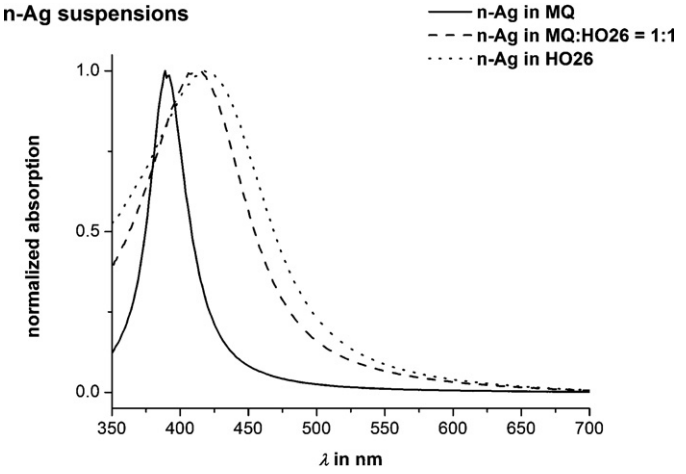

Fig. 1. UV–vis absorption spectra of n-Ag suspensions in different matrices.

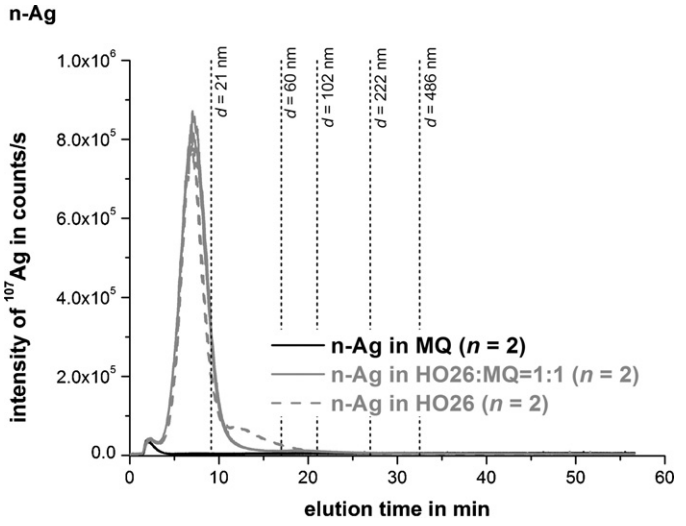

Fig. 2. AF4-fractograms of the three initial n-Ag suspensions (ICP-MS intensity of ^{107}Ag). Elution times and particle sizes of polystyrene standards are added as dashed lines.

off: 300 Da; spacer thickness: 350 μm; injection volume: 100 μL; detector flow: 0.3 mL/min). Each sample was injected in duplicate. Cross flow rate was kept constant at 80% for the first 4 min of fractionation and then exponentially decreased (60% after 8 min, 50%

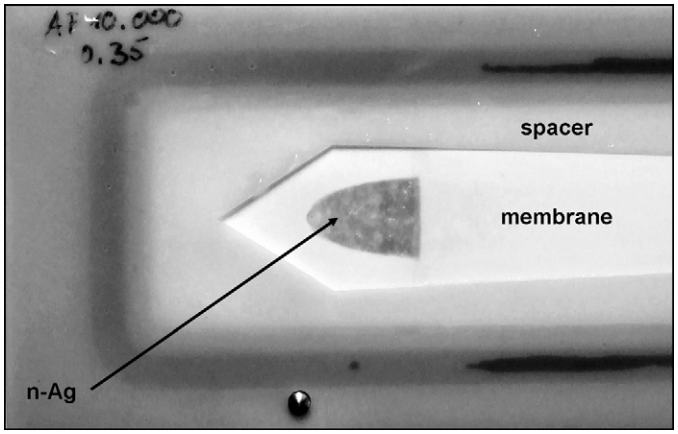

Fig. 3. AF4 channel with deposited n-Ag particles from the experiment without NOM addition.

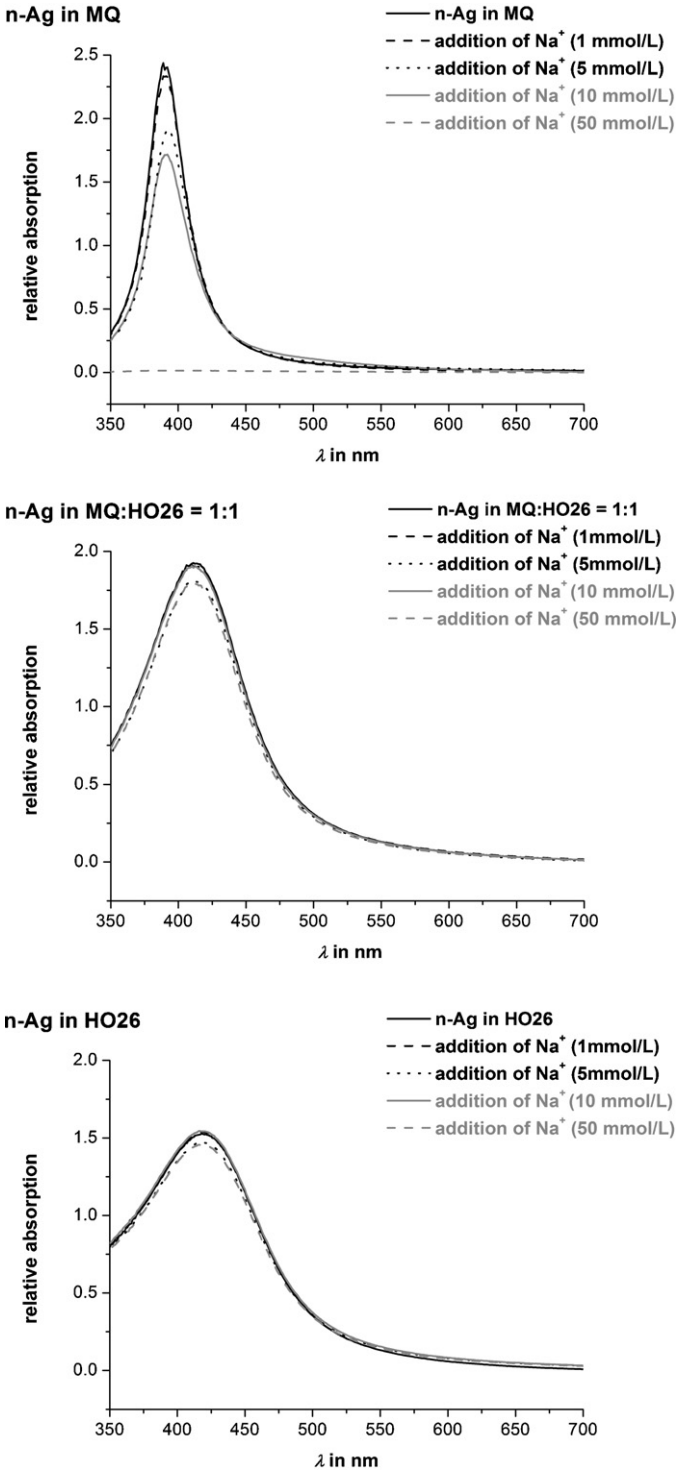

Fig. 4. UV–vis spectra of n-Ag in MQ (top), in a mixture of brown water (HO26) and MQ (ρ(DOC) = 9.0 mg/L; middle), and in HO26 (ρ(DOC) = 17.8 mg/L; bottom) at different concentrations of $NaNO_3$.

after 9.75 min, 10% after 29 min). This method has turned out to be well suited for the separation of nanoparticles and colloids [9,42]. Polystyrene standards were used for size calibration of the AF4 system (Duke Scientific; particle diameters: 21 ± 1.5 nm, 60 ± 2.5 nm, 102 ± 3 nm, 222 ± 6 nm, 486 ± 5 nm).

on-line detectors after the separation channel were: UV–vis (UVVIS-206, Linear Instruments) and an ICP-MS (ELAN 6000, Perkin Elmer). Detection of n-Ag particles and

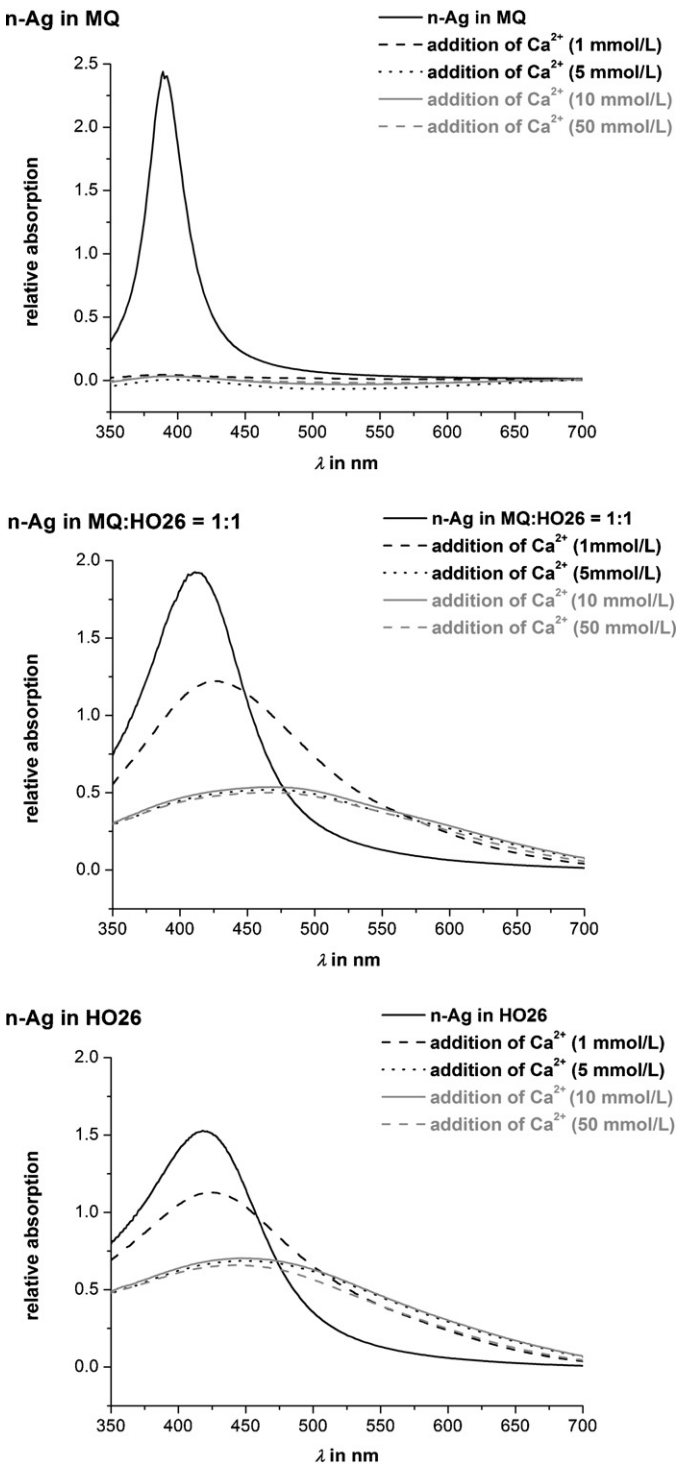

Fig. 5. UV–vis spectra of n-Ag in MQ (top), in a mixture of brown water (HO26) and MQ (ρ(DOC) = 9.0 mg/L; middle), and in HO26 (ρ(DOC) = 17.8 mg/L; bottom) at different concentrations of $Ca(NO_3)_2$.

polystyrene standards was done at λ = 400 nm and at λ = 254 nm, respectively.

3. Results and discussion

3.1. Characterization of initially synthesized n-Ag suspensions

The initially synthesized n-Ag suspensions have been stable for a few months. For n-Ag/MQ, this is likely due to the presence of BH_4^- as capping agent and a resulting electrostatic stabilization due to the repulsive electrostatic forces: for n-Ag/MQ particles negative values for the electrophoretic mobility and thus the zeta potential could be obtained (Table 1). This behaviour can be explained by the adsorption of BH_4^- anions onto the n-Ag particles [12,39,43]. In the presence of NOM, the zeta potential of the n-Ag particles was also negative, which fits to the observations on other nanoparticles (ZnO, NiO, TiO_2, Fe_2O_3 and SiO_2) [44]. In our case, we assume that both remaining BH_4^- and adsorbed NOM molecules lead to the negative zeta potential and thus, to both a charge and steric stabilization (see Section 1) of the n-Ag suspensions.

Our hypothesis of NOM adsorption on the n-Ag particles also seems to be valid regarding the changing hydrodynamic diameter d_h in the presence of NOM. Batch DLS measurements revealed a higher d_h (number mean values) for the initially synthesized n-Ag particles in the presence of NOM than in its absence (Table 1). Increase of d_h in the presence of NOM can be explained by the adsorption of NOM molecules on the n-Ag particles ("coating"), which has also been reported by Sánchez-Cortés et al. [45]. Iron oxide nanoparticles suspensions also showed an increase of particle size when NOM concentration in the suspensions was increased [46]. Even though it is attractive to assume a positive correlation between the NOM concentration in the solution and the particle size in the n-Ag suspension, the correlation might be limited to a special concentration range, which has to be elucidated in further experiments.

The hypothesis that n-Ag particles are coated by NOM, that they increase in particle size in the presence of NOM and that they change their properties has also been supported by the UV–vis absorption spectra of the three initial n-Ag suspensions n-Ag/MQ, n-Ag/MQ-HO26 and n-Ag/HO26 (Fig. 1) and their different separation behaviour during AF^4 fractionation (Fig. 2):

- In the presence of NOM, a shift of the absorption maximum from λ = 390 nm (n-Ag/MQ) to higher wavelengths (n-Ag/MQ-HO26: λ = 410 nm, n-Ag/HO26: 420 nm) could be observed. As mentioned in Section 1, a shift towards higher wavelengths has been prognosed as an attractive indicator for particle growth, in this case due to the adsorption of NOM molecules onto the n-Ag particles [30,33,35,47,48]. For the two suspensions containing NOM, a similar absorption maximum could be obtained, which is in good agreement with the similar values for d_h of these samples obtained by DLS measurement and in AF^4 experiments (see Section 3.2). Furthermore, a peak broadening could be observed for the n-Ag suspensions containing NOM. This behaviour can be attributed to an increasing polydispersity of the samples caused by the formation of aggregates between NOM and n-Ag. This finding will further be considered in the discussion of the results obtained by AF^4 measurements.
- In Fig. 2, fractograms for the three initial n-Ag suspensions are shown together with the mean elution times of the particle standards used for calibration. During AF^4 fractionation, the n-Ag/MQ particles showed a different separation behaviour than the n-Ag particles in the presence of NOM. n-Ag/MQ particles exhibited a strong interaction with the membrane material resulting in a poor recovery as indicated by the significantly lower intensity for Ag (ICP-MS) and UV–vis (not shown here). The n-Ag particles were visible after fractionation on the membrane (Fig. 3). These findings could also be observed using other membrane materials such as regenerated cellulose and using larger n-Ag particles synthesized in MQ. This problem of nanoparticle–membrane interaction has already been described in the literature [29].

In contrast, n-Ag suspensions containing NOM could be separated, with particle diameters mostly being smaller than 21 nm (peak for both suspensions at approximately 7 min). Applying a

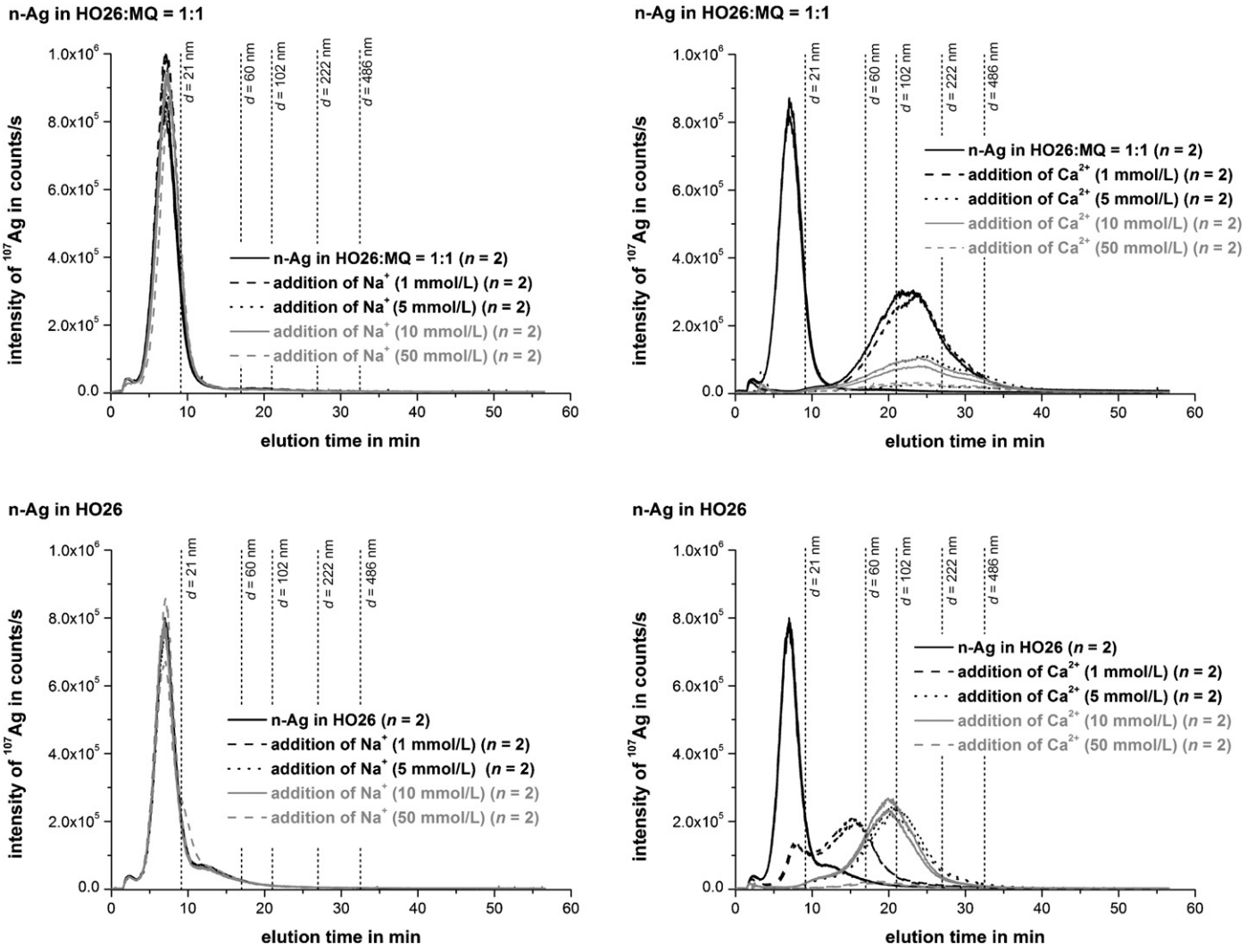

Fig. 6. AF^4-fractograms for n-Ag suspensions in the presence of NOM and addition of $NaNO_3$ or $Ca(NO_3)_2$ (ICP-MS intensity of ^{107}Ag).

non-linear calibration curve (exponentially decreasing cross flow profile) results in calculated d_h in the range of 9 nm, which is in good agreement with the similar DLS results obtained for both n-Ag suspensions. It is interesting to note that for n-Ag/HO26 samples, a second fraction containing Ag with particle sizes between 20 and 60 nm could be observed (see also Figs. 6 and 7). This indicates that to a low extent, also larger aggregates containing Ag are already formed in the presence of NOM. These findings are also consistent with the peak broadening which could be observed in the UV–vis spectra of these suspensions.

The fact that there were no difficulties in obtaining fractograms of n-Ag in NOM-rich matrices supports the interpretation of our results that NOM significantly changes the surface properties of n-Ag. Under the conditions applied during the AF^4 separation (here: neutral pH value), the PES membrane has a negative surface charge [49]. The n-Ag particles in the different initial suspensions also showed a negative zeta potential. Hence, due to the resulting repulsive electrostatic forces, no significant problems in the separation had been expected. The contradictive effects can be explained by assuming sterical hindrance of the NOM-coated n-Ag particles to reach the membrane material, especially during the injection and focussing step of AF^4 fractionation. In contrast, without NOM, n-Ag particles are pressed onto the membrane material during the injection and focussing step, resulting in a stronger interaction with the membrane. It could not be answered finally whether the assumed BH_4^- coating of the bare n-Ag/MQ particles might also react with the membrane material or not. For the investigation of details of these interactions, experiments with different eluent compositions and electron-microscopic studies are on the way

3.2. Stability of n-Ag suspensions

Figs. 4 and 5 show UV–vis spectra of the n-Ag suspensions at different concentrations of $NaNO_3$ and $Ca(NO_3)_2$. The spectra indicate that n-Ag suspensions in the presence of NOM remained more stable when calcium or sodium salts were added, whereas n-Ag particles in the absence of NOM were rapidly destabilized as indicated by a decreasing absorption at $\lambda \approx 400$ nm. This behaviour is supposed to be due to the compression of the electrical double layer at increasing ionic strength resulting in particle aggregation and precipitation. The molar concentration necessary to reach a destabilization effect for n-Ag suspensions in the absence of NOM is much lower for calcium than for sodium which can be attributed to the bivalence of Ca^{2+} and the resulting higher ionic strength [8].

Obviously, presence of NOM improved the stability of dispersed n-Ag due to surface coating of the particles and steric and charge stabilization [29]. Similar findings have been reported for the stability of TiO_2 nanoparticles [50]. After addition of Na^+, n-Ag suspensions showed no significant changes regarding their spectral absorption behaviour, which indicates that the suspensions

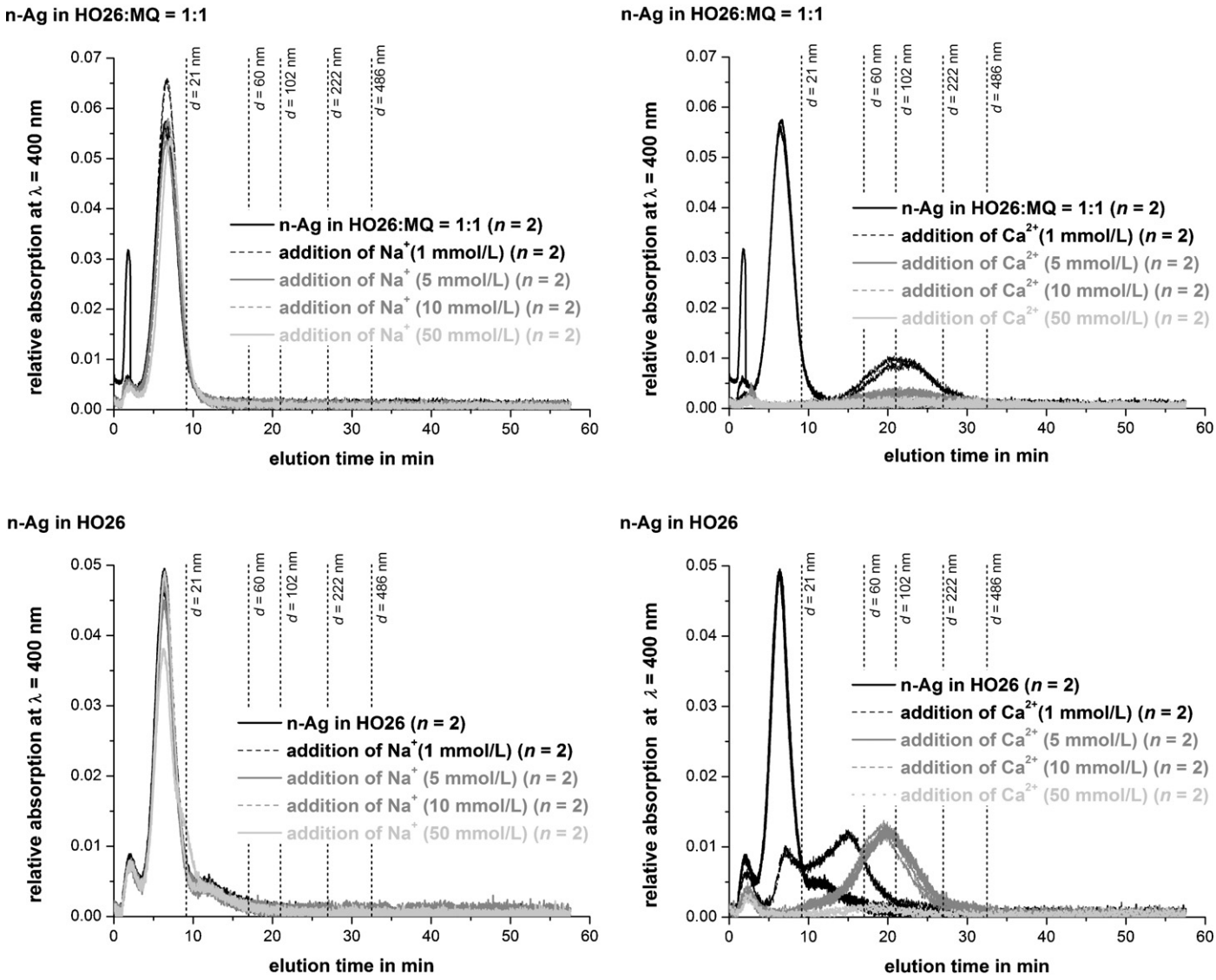

Fig. 7. AF^4-fractograms for n-Ag suspensions in the presence of NOM and addition of $NaNO_3$ or $Ca(NO_3)_2$ (spectral absorption detection at $\lambda = 400$ nm).

were not significantly destabilized. Addition of divalent Ca^{2+} ions (resulting in a higher ionic strength) to the aqueous n-Ag samples containing NOM resulted in suspensions which were still stable, but showed changes in colour and particle size distribution as indicated by the shift of the absorption peak maximum towards higher wavelengths and the peak broadening of the UV–vis spectra. The presence of Ca^{2+} ions has two effects: it leads (1) to the electrostatic destabilization of the particle system and (2) to the agglomeration of organic macromolecules with Ca^{2+} acting as bridging cation [51,52]. As a consequence, larger aggregates are formed and sediment as indicated by decreasing absorption intensities at increasing Ca^{2+} concentrations. However, due to the steric stabilization of the NOM-coated n-Ag particles in the presence of NOM, some of these aggregates are still small enough to stay dispersed in suspension.

In order to follow the aggregation of n-Ag suspensions in detail and to characterize the aggregates, AF^4 coupled with UV–vis detection and ICP-MS was used. Use of DLS for characterization of these aggregates has shown to be problematic as some of the resulting suspensions have been highly polydisperse.

In Figs. 6 and 7, AF^4-fractograms of n-Ag/MQ-HO26 and n-Ag/HO26 suspensions after addition of sodium or calcium (50 mmol/L) are shown (*on-line* detection of Ag by means of ICP-MS and UV–vis at 400 nm). Generally, there is a good agreement between the fractograms obtained using UV–vis and ICP-MS detection (except for the void peak signal at an elution time of 2 min).

Addition of $NaNO_3$ to both n-Ag suspensions did not significantly change their particle size distribution (particle diameter < 21 nm, calculated value $d_h \approx 9$ nm). These findings for the particle size are in good accordance with the results from batch DLS measurements and the UV–vis investigations. Addition of $Ca(NO_3)_2$ leads to the formation of larger aggregates containing n-Ag, which, however, were still stable (median particle diameter of 90–150 nm). The results obtained by AF^4 experiments validate the findings obtained by UV–vis spectroscopy as an independent method. Additionally to the information obtained by UV–vis spectroscopy, coupling of AF^4 with UV–vis and ICP-MS provides sound and reproducible information on the particle size distribution and the chemical composition of the nanoparticles investigated. Furthermore, the aggregation behaviour of n-Ag suspensions could be followed in detail when ionic strength was increased step by step. It could be observed that for the n-Ag/HO26 suspensions, n-Ag particles gradually form larger aggregates at increasing Ca^{2+} concentration, whereas for n-Ag/MQ-HO26 suspensions, larger

aggregates were already formed at $c(Ca^{2+}) = 1$ mmol/L as shown in Figs. 6 and 7.

For both suspensions, at a concentration of $c(Ca^{2+}) = 50$ mmol/L, the recovery of n-Ag particles and their agglomerates was poor, which indicates the formation of aggregates or flocs which are too large to stay in suspension and thus sediment in the sample tube. Characterization of the aggregates in will need electron-microscopic methods.

As indicated by the similar results obtained applying ICP-MS or UV–vis detection after AF^4 separation, UV–vis absorption has also turned out to be well-suited to detect n-Ag particles and their stability in these model systems (Fig. 7). Even though it is an attractive and cost efficient method compared with ICP-MS detection, the investigation of environmental samples with unknown constituents will still need ICP-MS detection to identify the chemical composition of the (nano)particles.

We are aware of the fact that the particle standards used for our calibration of the AF^4 system might show different separation behaviour than the n-Ag particles used in the experiment. However, this is a general problem in AF^4 calibration for even Ag particle standards are likely to behave differently than the Ag particles in the experimental sample depending on their specific surface modification. As a consequence, for further studies, *on-line* detection of particle size (e.g. dynamic and/or static light scattering) is highly attractive [53].

4. Conclusions

The results shown indicate clearly that NOM significantly influences the particle size distribution, the stability and the surface properties of n-Ag in the aqueous phase, which will also crucially affect the transport behaviour and the toxicity of n-Ag in aquatic systems [54]. In the presence of NOM, n-Ag suspensions are still stable at considerable ionic strength, which will facilitate their transport in environmental systems.

Coupling of AF^4 with UV–vis and ICP-MS allowed the highly sensitive detection of n-Ag directly in liquid samples, providing simultaneous information on the particle size distribution and on the chemical composition of the particles. This method has turned out to be a promising tool for the highly sensitive detection and quantification of ENP in environmental systems. However, it is a key task for the future to further develop this method, especially regarding the interactions between nanoparticles and membrane material.

Acknowledgements

The authors thank Anne Ruehl for their fine experimental work and the KIT competence area “Earth and Environment” for financial support.

References

[1] DIN CEN ISO/TS 27687, Deutsches Institut für Normung e.V. (German Institute for Standardization) (DIN), 2008.
[2] E 2456-06, Standard Terminology Relating to Nanotechnology, American Society for Testing and Materials, 2009.
[3] M. Auffan, J. Rose, J.-Y. Bottero, G.V. Lowry, J.-P. Jolivet, M.R. Wiesner, Nat. Nanotechnol. 4 (2009) 634.
[4] R.J. Aitken, M.Q. Chaudhry, A.B.A. Boxall, M. Hull, Occup. Med. 56 (2006) 300.
[5] M.R. Wiesner, G.V. Lowry, K.L. Jones, M.F.J. Hochella, E. Casman, E.S. Bernhardt, Environ. Sci. Technol. 43 (2009) 6458.
[6] M.C. Roco, Environ. Sci. Technol. 39 (2005) 106A.
[7] Q. Chaudhry, M. Scotter, J. Blackburn, B. Ross, A. Boxall, L. Castle, R. Aitken, R. Watkins, Food Addit. Contam. 25 (2008) 241.
[8] F.H. Frimmel, M. Delay, in: F.H. Frimmel, R. Niessner (Eds.), Nanoparticles in the Water Cycle: Properties, Analysis and Environmental Relevance, Springer, Berlin, 2010, p. 1.
[9] M. Delay, L.A.T. Espinoza, G. Metreveli, F.H. Frimmel, in: F.H. Frimmel, R. Niessner (Eds.), Nanoparticles in the Water Cycle: Properties, Analysis and Environmental Relevance, Springer, Berlin, 2010, p. 139.
[10] R. Kaegi, B. Sinnet, S. Zuleeg, H. Hagendorfer, E. Mueller, R. Vonbank, M. Boller, M. Burkhardt, Environ. Pollut. 158 (2010) 2900.
[11] S.A. Blaser, M. Scheringer, M. MacLeod, K. Hungerbühler, Sci. Total Environ. 390 (2008) 396.
[12] Z.-J. Jiang, C.-Y. Liu, L.-W. Sun, J. Phys. Chem. B 109 (2005) 1730.
[13] D.P. Chen, X.L. Qiao, X.L. Qiu, J.G. Chen, J. Mater. Sci. 44 (2009) 1076.
[14] T.M. Benn, P. Westerhoff, Environ. Sci. Technol. 42 (2008) 4133.
[15] L. Geranio, M. Heuberger, B. Nowack, Environ. Sci. Technol. 43 (2009) 8113.
[16] E. Navarro, F. Piccapietra, B. Wagner, F. Marconi, R. Kaegi, N. Odzak, L. Sigg, R. Behra, Environ. Sci. Technol. 42 (2008) 8959.
[17] N.R. Panyala, E.M. Pena-Mendez, J. Havel, J. Appl. Biomed. 6 (2008) 117.
[18] B. Nowack, T.D. Bucheli, Environ. Pollut. 150 (2007) 5.
[19] N.C. Mueller, B. Nowack, Environ. Sci. Technol. 42 (2008) 4447.
[20] P.J.J. Alvarez, V. Colvin, J. Lead, V. Stone, ACS Nano 3 (2009) 1616.
[21] S.D. Faust, O.M. Aly, Chemistry of Natural Waters, Ann Arbor Science Publishers Michigan, 1981, p. 400.
[22] R.F. Christman, E.T. Gjessing (Eds.), Aquatic and Terrestrial Humic Materials, Ann Arbor Science, Michigan, 1983, p. 538.
[23] F.H. Frimmel, G. Abbt-Braun, K.G. Heumann, B. Hock, H.-D. Lüdemann, M. Spiteller (Eds.), Refractory Organic Substances in the Environment, WILEY-VCH, Weinheim, 2002, p546.
[24] A.J. Pelley, N. Tufenkji, J. Colloid Interface Sci. 321 (2008) 74.
[25] R.L. Johnson, G.O.B. Johnson, J.T. Nurmi, P.G. Tratnyek, Environ. Sci. Technol. 43 (2009) 5455.
[26] D.H. Napper, J. Colloid Interface Sci. 58 (1977) 390.
[27] C. Lourenco, M. Teixeira, S. Simões, R. Gaspar, Int. J. Pharm. 138 (1996) 1.
[28] S. Diegoli, A.L. Manciulea, S. Begum, I.P. Jones, J.R. Lead, J.A. Preece, Sci. Total Environ. 402 (2008) 51.
[29] S.A. Cumberland, J.R. Lead, J. Chromatogr. A 1216 (2009) 9099.
[30] C.S. Seney, B.M. Gutzman, R.H. Goddard, J. Phys. Chem. C 113 (2008) 74.
[31] D.L. Van Hyning, C.F. Zukoski, Langmuir 14 (1998) 7034.
[32] J.A. Creighton, C.G. Blatchford, M.G. Albrecht, J. Chem. Soc. 2 (1979) 790.
[33] S. Link, M.A. El-Sayed, J. Phys. Chem. B 103 (1999) 4212.
[34] A. Slistan-Grijalva, R. Herrera-Urbina, J.F. Rivas-Silva, M. Ávalos-Borja, F.F. Castillón-Barraza, A. Posada-Amarillas, J. Phys. E 27 (2005) 104.
[35] V.S. Lebedev, A.G. Vitukhnovsky, A. Yoshida, N. Kometani, Y. Yonezawa, Colloid Surf. A 326 (2008) 204.
[36] M. Baalousha, F.V.D. Kammer, M. Motelica-Heino, P. Le Coustumer, J. Chromatogr. A 1093 (2005) 156.
[37] S. Dubascoux, I.L. Hecho, M. Hassellov, F.V.D. Kammer, M.P. Gautier, G. Lespes, J. Anal. Atom. Spectrom. 25 (2010) 613.
[38] E. Bolea, F. Laborda, J.R. Castillo, Anal. Chim. Acta 661 (2010) 206.
[39] K. Song, S. Lee, T. Park, B. Lee, Korean J. Chem. Eng. 26 (2009) 153.
[40] G. Abbt-Braun, U. Lankes, F. Frimmel, Aquat. Sci. 66 (2004) 151.
[41] H. Weingärtner, E.U. Franck, G. Wiegand, N. Dahmen, G. Schwedt, F.H. Frimmel, B.C. Gordalla, K. Johannsen, R.S. Summers, W. Höll, M. Jekel, R. Gimbel, R. Rautenbach, W.H. Glaze, Water Ullmann’s Encyclopedia of Industrial Chemistry, 2000.
[42] G. Metreveli, Kolloidale Wechselwirkungen und kolloidgetragener Transport von Metall(oid)en in porösen Medien, Dissertation, Karlsruhe, 2008.
[43] A.M.E. Badawy, T.P. Luxton, R.G. Silva, K.G. Scheckel, M.T. Suidan, T.M. Tolaymat, Environ. Sci. Technol. 44 (2010) 1260.
[44] Y. Zhang, Y. Chen, P. Westerhoff, J. Crittenden, Water Res. 43 (2009) 4249.
[45] S. Sánchez-Cortés, O. Francioso, C. Ciavatta, J.V. García-Ramos, C. Gessa, J. Colloid Interface Sci. 198 (1998) 308.
[46] M. Baalousha, A. Manciulea, S. Cumberland, K. Kendall, J.R. Lead, Environ. Toxicol. Chem. 27 (2008) 1875.
[47] S.L. Smitha, K.M. Nissamudeen, D. Philip, K.G. Gopchandran, Spectrochim. Acta A 71 (2008) 186.
[48] T. Dadosh, Mater. Lett. 63 (2009) 2236.
[49] L. Braeken, B. Bettens, K. Boussu, P. Van der Meeren, J. Cocquyt, J. Vermant, B. Van der Bruggen, J. Membr. Sci. 279 (2006) 311.
[50] F. Domingos, N. Tufenkji, K.J. Wilkinson, Environ. Sci. Technol. 43 (2009) 1282.
[51] K.L. Chen, M. Elimelech, J. Colloid Interface Sci. 309 (2007) 126.
[52] N.B. Saleh, L.D. Pfefferle, M. Elimelech, Environ. Sci. Technol. 44 (2010) 2412.
[53] A. Zattoni, D.C. Rambaldi, P. Reschiglian, M. Melucci, S. Krol, A.M.C. Garcia, A. Sanz-Medel, D. Roessner, C. Johann, J. Chromatogr. A 1216 (2009) 9106.
[54] J. Fabrega, S.R. Fawcett, J.C. Renshaw, J.R. Lead, Environ. Sci. Technol. 43 (2009) 7285.